IEEE Access
Multidisciplinary | Rapid Review | Open Access Journal

Received December 21, 2019, accepted January 19, 2020, date of publication January 22, 2020, date of current version February 6, 2020.

*Digital Object Identifier 10.1109/ACCESS.2020.2968575*

# The Transfer Matrix Method: Analysis of Nonuniform Multiport Systems

**J. A. BRANDÃO FARIA, (Fellow, IEEE)**
Instituto de Telecomunicações, Instituto Superior Técnico, University of Lisbon, 1049-001 Lisbon, Portugal
e-mail: brandao.faria@tecnico.ulisboa.pt

This work was supported in part by the FCT/MCTES through national funds, and in part by EU funds under Project UIDB/EEA/50008/2020.

**ABSTRACT** A ubiquitous tool in science, physics, and engineering at large, the transfer matrix method (TMM) is particularly suited to deal with complex nonuniform systems (NUS). In the field of electrical engineering, the method is employed in a variety of disciplines that span the electromagnetic spectrum, from power frequencies through RF, millimeter-waves, and terahertz. In this work, three nested goals are pursued. The first is to present a general comprehensive review of the transfer matrix method utilizing two distinct languages: the state space (via the matricant) and the modal analysis (via matrix diagonalization). The second goal, focused on electrical engineering issues, is the application of TMM to the interdisciplinary theme of nonuniform multiconductor transmission lines (MTL) −a good example of a complex reciprocal multiport system. The third goal is to offer the reader novel research results in the context of MTL analysis. Making use of a simple microwave stripline-coupler structure new theoretical results are presented showing that, in some cases, load impedance matching of nonuniform MTLs, using only passive components, may not be physically possible (negative resistors being required), even if the global NUS is longitudinally and transversally symmetric, with or without losses.

**INDEX TERMS** Impedance matching, matricant, modal analysis, multiconductor transmission lines, nonuniform structures, reciprocal multiport systems, state-space approach, transfer matrix method.

## I. INTRODUCTION

All physical structures, natural or artificial/man-made, are nonuniform systems in the sense that their 3D volume description includes periodic, quasiperiodic or nonperiodic variations at least in one direction ($x$, $y$, or $z$), either in terms of topology or medium properties.

The transfer matrix method (TMM) is a key tool [1]–[38] in science, physics, engineering, and technology research when nonuniform structures (NUS) are at play; the method being specially fitted for the frequency-domain analysis of linear time-invariant systems with stratified material media and/or layered geometries.

The subject of NUS/TMM is interdisciplinary. It turned out a very important area of research in electrical engineering [14]–[28] owing to its impact on almost all of its subareas: control, electromagnetics, microwaves, optics, power systems, telecommunications, etc. Other engineering fields like acoustics, bio, civil, fluids, materials, mechanics, etc. also employ TMM [29]–[35], even genetic science is using TMM in DNA research [36]–[38].

As mentioned, the transfer matrix method is well suited for the frequency-domain analysis of NUS, especially when the components of the NUS are lossy and have dispersive behavior.

Time-domain results can be retrieved from their spectral counterparts via Fourier transforms. Albeit very accurate, ordinary time-domain→frequency-domain→time-domain methods may require long computation times. CPU times can be greatly reduced by opting for conventional finite-difference time-domain algorithms, but, unfortunately, these are not unconditionally stable, and do not work well with dispersive media.

This article is organized into seven sections, the first of which is introductory. The four following sections are dedicated to the review of the transfer matrix method. The sixth section, focused on a concrete application, combines review and research. The article ends with a conclusion section and a bibliographic list whose references cover the timespan 1888 to 2019.

The associate editor coordinating the review of this manuscript and approving it for publication was Flavia Grassi.

Section II presents the frequency-domain theoretical framework for the general analysis of nonuniform multiport structures, where the state-space approach, or 'matricant', is utilized to obtain/compute the structure's transfer matrix in the form of a convergent series expansion. The results offered in Section II are particularized in Section III to the simple, but important, case of uniform multiport structures, and, in that context, the 'matricant' approach is confronted with the rival method of 'diagonalization' (eigenproblem).

The well-known segmentation technique is briefly addressed in Section IV. Useful and rather intuitive the technique consists of replacing the nonuniform multiport structure by the chain connection of a large number of small uniform multiport cells, the global transfer matrix being obtained by continuous multiplication of the cells' individual transfer matrices.

The topic of extracting the transfer matrix of an NUS black-box from experimental measurements is touched upon in Section V, taking account of the properties peculiar to the transfer matrix.

Finally, in Section VI (the longest one), the utilization of the transfer matrix method is concretized and illustrated with the electrical engineering subject of multiconductor transmission-line structures (MTL) —a cross-disciplinary theme whose interest spans the whole spectrum, from 60 Hz long-length power lines to terahertz tiny optical devices. Section VI comprises three subsections. The first is aimed at the determination of the transfer matrix of nonuniform MTL problems; the second to their solutions via modal analysis. Dedicated to novel research results, the last subsection deals with the curious example of a microwave stripline coupler with two cascaded halves imperfectly connected, where load matching terminations may turn out to be unfeasible.

## II. THEORETICAL BACKGROUND

The complexity of an NUS depends on its degrees of freedom, determined from the number $n$ of pairs of scalar state-space variables required for its complete description, for example: displacement and force components, pressure and velocity components, tension and torque components, voltages and currents, electric-field and magnetic-field components, etc.

Consider a linear passive nonuniform structure of length $l$, whose internal constitution varies along the $x$-coordinate, and whose complexity requires $2n$ scalar state variables for its characterization: $p_k$ and $q_k$ (for $k = 1 \cdots n$), all of them depending on $x$ and $t$ coordinates.

Assuming, without loss of generality that $p_k$ and $q_k$ are time-harmonic, of frequency $\omega$ $(= 2\pi f)$, one can write

$$\begin{cases} p_k(x,t) = \Re\left\{\bar{P}_k(x)e^{j\omega t}\right\} \\ q_k(x,t) = \Re\left\{\bar{Q}_k(x)e^{j\omega t}\right\} \end{cases} \tag{1}$$

where $\bar{P}_k$ and $\bar{Q}_k$ are phasor representations of $p_k$ and $q_k$.

The transfer matrix $\mathbf{T}_l$ (also known by the name of **ABCD** matrix, transmission matrix, or chain matrix) is a complex non-symmetric $2n \times 2n$ matrix that permits the calculation of the phasor pairs $(\bar{P}_k,\ \bar{Q}_k)$ at the output end, $x = l$, from those at the input end, $x = 0$, for all values of $k$, that is

$$\boldsymbol{\Psi}_l = \mathbf{T}_l \boldsymbol{\Psi}_0, \quad \mathbf{T}_l = \begin{bmatrix} \mathbf{A} & \mathbf{B} \\ \mathbf{C} & \mathbf{D} \end{bmatrix} \tag{2}$$

where, for $x \in [0\ ,\ l]$,

$$\boldsymbol{\Psi}_x = \boldsymbol{\Psi}(x) = \mathbf{T}(x)\Psi_0 = \begin{bmatrix} \mathbf{P}_x \\ \mathbf{Q}_x \end{bmatrix} \tag{3}$$

and

$$\mathbf{P}_x = \begin{bmatrix} \bar{P}_1(x) \\ \bar{P}_2(x) \\ \vdots \\ \bar{P}_n(x) \end{bmatrix}, \quad \mathbf{Q}_x = \begin{bmatrix} \bar{Q}_1(x) \\ \bar{Q}_2(x) \\ \vdots \\ \bar{Q}_n(x) \end{bmatrix} \tag{4}$$

Assuming (in addition to passivity) that the NUS is also a reciprocal structure, its transfer matrix will be unimodular

$$\forall x: \ \det \mathbf{T}(x) = 1 \tag{5}$$

The transfer matrix usually shows up in connection with first-order linear homogeneous differential matrix equations [28], [39]–[41], of the type

$$\frac{d}{dx}\boldsymbol{\Psi}(x) = \mathbf{S}(x)\boldsymbol{\Psi}(x) \tag{6}$$

where $\mathbf{S}$ often bears the name of state transition matrix.

Integration of (6) from $x = 0$ to $x = l$ gives

$$\boldsymbol{\Psi}_{(x=l)} = \boldsymbol{\Psi}_0 + \int_0^l \mathbf{S}(x)\boldsymbol{\Psi}(x)dx \tag{7}$$

Substituting $(\mathbf{T}(x)\boldsymbol{\Psi}_0)$ for $\boldsymbol{\Psi}(x)$ into (7) yields

$$\mathbf{T}(l) = \mathbf{1} + \int_0^l \mathbf{S}(x)\mathbf{T}(x)dx \tag{8}$$

where $\mathbf{1}$ is the identity matrix.

Next, by endlessly substituting $\mathbf{T}(l)$, with $l$ replaced by $x$, in the right-hand side of (8), we obtain the solution for $\mathbf{T}_l$ in terms of nested integrals of $\mathbf{S}(x)$,

$$\mathbf{T}_l = \mathbf{1} + \int_0^l \mathbf{S}(x) \times \left(\mathbf{1} + \int_0^x \mathbf{S}(x_1)\left(\mathbf{1} + \int_0^{x_1} \mathbf{S}(x_2)\left(\mathbf{1} + \int \cdots\right)dx_2\right)dx_1\right)dx \tag{9}$$

or as an infinite series

$$\mathbf{T}_l = \begin{bmatrix} \mathbf{A} & \mathbf{B} \\ \mathbf{C} & \mathbf{D} \end{bmatrix} = \mathbf{1} + \Upsilon_1 + \Upsilon_2 + \Upsilon_3 + \cdots = \sum_{m=0}^{\infty} \Upsilon_m \tag{10}$$

where $\Upsilon_0 = \mathbf{1}$, and

$$\begin{cases} \Upsilon_1(l) = \int_0^l \mathbf{S}(x)\,dx \\ \Upsilon_2(l) = \int_0^l \mathbf{S}(x) \overbrace{\left(\int_0^x \mathbf{S}(x_1)dx_1\right)}^{\Upsilon_1(x)} dx \\ \Upsilon_3(l) = \int_0^l \mathbf{S}(x) \overbrace{\left(\int_0^x \mathbf{S}(x_1)\left(\int_0^{x_1} \mathbf{S}(x_2)dx_2\right)dx_1\right)}^{\Upsilon_2(x)} dx \\ \quad\vdots \\ \Upsilon_m(l) = \int_0^l \mathbf{S}(x)\Upsilon_{m-1}(x)\,dx \end{cases} \tag{11}$$

The solution in (10)-(11), known in Linear Algebra by the matricant [32], [39], [40], is an absolutely uniformly convergent series expansion. The series, firstly obtained by Peano, was later developed by Baker and, modernly, by Magnus, [28], [42]–[48].

In addition to (5), the $n \times n$ submatrices of $\mathbf{T}_l$ in (10) satisfy the following properties, [20],

$$\begin{cases} \mathbf{A}\mathbf{B}^T - \mathbf{B}\mathbf{A}^T = \mathbf{D}^T\mathbf{B} - \mathbf{B}^T\mathbf{D} = \mathbf{0} \\ \mathbf{D}\mathbf{C}^T - \mathbf{C}\mathbf{D}^T = \mathbf{A}^T\mathbf{C} - \mathbf{C}^T\mathbf{A} = \mathbf{0} \\ \mathbf{A}\mathbf{D}^T - \mathbf{B}\mathbf{C}^T = \mathbf{D}^T\mathbf{A} - \mathbf{B}^T\mathbf{C} = \mathbf{1} \end{cases} \tag{12}$$

$$\begin{bmatrix} \mathbf{A} & \mathbf{B} \\ \mathbf{C} & \mathbf{D} \end{bmatrix}^{-1} = \begin{bmatrix} \mathbf{D} & -\mathbf{C} \\ -\mathbf{B} & \mathbf{A} \end{bmatrix}^T \tag{13}$$

where superscript $T$ denotes matrix transposition.

We can see from (12) that one of the four submatrices of $\mathbf{T}_l$ is redundant, for it can be found from the remaining three. For example, given $\mathbf{A}, \mathbf{B},$ and $\mathbf{C}$, we can find $\mathbf{D}$ from

$$\mathbf{D}^T = \mathbf{A}^{-1}(\mathbf{1} + \mathbf{B}\mathbf{C}^T) = (\mathbf{1} + \mathbf{B}^T\mathbf{C})\mathbf{A}^{-1} \tag{14}$$

If the nonuniform structure is periodical with period $l$, that is, if it is made of the chain connection of $N$ identical cells, then the overall transfer matrix will simply be given by the $N^{th}$ power of $\mathbf{T}_l$.

## III. UNIFORM STRUCTURES

For the particular case of uniform structures, where $\mathbf{S}$ is $x$-independent, the calculation of the terms of the series expansion in (11) is not difficult, yielding

$$\begin{cases} \Upsilon_1(l) = \mathbf{S}l \\ \Upsilon_2(l) = \frac{1}{2}(\mathbf{S}l)^2 \\ \Upsilon_3(l) = \frac{1}{6}(\mathbf{S}l)^3 \\ \quad\vdots \\ \Upsilon_m(l) = \frac{1}{m!}(\mathbf{S}l)^m \end{cases} \tag{15}$$

The terms appearing in (15) are quite well-known; they are the terms of Taylor's series for the exponential function. This leads to the conclusion that the transfer matrix $\mathbf{T}_l$ is the exponential function of $(\mathbf{S}l)$

$$\mathbf{T}_l = \begin{bmatrix} \mathbf{A} & \mathbf{B} \\ \mathbf{C} & \mathbf{D} \end{bmatrix} = \sum_{m=0}^{\infty} \frac{(\mathbf{S}l)^m}{m!} = e^{\mathbf{S}l} \tag{16}$$

In the case of uniform structures, the results in (12)-(13) simplify, [20], yielding

$$\begin{cases} \mathbf{A} = \mathbf{D}^T, \quad \mathbf{B} = \mathbf{B}^T, \quad \mathbf{C} = \mathbf{C}^T \\ \mathbf{A}\mathbf{B} = \mathbf{B}\mathbf{D}, \quad \mathbf{D}\mathbf{C} = \mathbf{C}\mathbf{A} \\ \mathbf{A}^2 - \mathbf{B}\mathbf{C} = \mathbf{D}^2 - \mathbf{C}\mathbf{B} = \mathbf{1} \end{cases} \tag{17}$$

$$\begin{bmatrix} \mathbf{A} & \mathbf{B} \\ \mathbf{C} & \mathbf{D} \end{bmatrix}^{-1} = \begin{bmatrix} \mathbf{A} & -\mathbf{B} \\ -\mathbf{C} & \mathbf{D} \end{bmatrix} \tag{18}$$

The properties listed now in (17) show that two of the four submatrices of $\mathbf{T}_l$ are redundant. The transfer matrix of uniform structures can be fully characterized by only two of its submatrices; for example, if $\mathbf{A}$ and $\mathbf{B}$ are known, then $\mathbf{C}$ and $\mathbf{D}$ will be determined from

$$\mathbf{C} = \mathbf{B}^{-1}(\mathbf{A}^2 - \mathbf{1}), \quad \mathbf{D} = \mathbf{A}^T \tag{19}$$

The matricant solution in (15)-(16) is an infinite summation which must be truncated at some order according to a prescribed accuracy level, the number of necessary terms depending on the frequency $\omega$.

A rather different strategy —diagonalization, [39], [40]—can be used to find the transfer matrix in (16). It involves the solution of an eingenvalue problem focused on the state transition matrix $\mathbf{S}$,

$$\mathbf{M}^{-1}\mathbf{S}\,\mathbf{M} = \mathbf{g} \text{ or } (\mathbf{S} - g_k\mathbf{1})\mathbf{m}_k = \mathbf{0} \tag{20}$$

where $\mathbf{g}$ is a diagonal matrix gathering the $g_k$ eigenvalues of $\mathbf{S}$ (for $k = 1$ to $2n$); the corresponding eigenvectors $\mathbf{m}_k$ being gathered in the transformation matrix $\mathbf{M}$.

Once (20) is solved, the exponential matrix function of $\mathbf{S}$ is readily obtained through, [39], [40],

$$\mathbf{T}_l = e^{\mathbf{S}l} = \mathbf{M}\,e^{\mathbf{g}l}\,\mathbf{M}^{-1} \tag{21}$$

where, like $\mathbf{g}$, matrix $e^{\mathbf{g}l}$ is $2n \times 2n$ diagonal

$$e^{\mathbf{g}l} = \begin{bmatrix} e^{-\gamma l} & \mathbf{0} \\ \mathbf{0} & e^{+\gamma l} \end{bmatrix} \tag{22}$$

where $\gamma$ and $e^{\gamma l}$ are $n \times n$ diagonal.

Exceptionally, when irregular multiple eigenvalues exist in $\gamma$, the diagonalization procedure in (20)-(21) fails, $\mathbf{M}$ is singular, and the transfer matrix $\mathbf{T}_l$ cannot be obtained from (21), [39], [40], [49]. However, the matricant procedure in (15)-(16) can always be implemented regardless of the presence of irregular eigenvalues.

The arrangement of the eigenvalues of $\mathbf{T}_l$ in (22), where they are gathered in two block-diagonal matrices

(inverse of each other), makes evident the property in (5) valid for reciprocal structures,

$$\det\ \mathbf{T}_l = \det\left(e^{\mathbf{g}l}\right) = \det\left(e^{+\gamma l}\right)\det\left(e^{-\gamma l}\right) = 1 \quad (23)$$

An immediate consequence of (20), (22) and (23) is that the $2n \times 2n$ diagonal matrix $\mathbf{g}$ is also partitioned in two $n \times n$ diagonal matrices,

$$\mathbf{g} = \begin{bmatrix} -\gamma & \mathbf{0} \\ \mathbf{0} & +\gamma \end{bmatrix} \rightarrow \mathrm{tr}(\mathbf{g}) = 0 \quad (24)$$

The traces of the similar matrices $\mathbf{g}$ and $\mathbf{S}$ ought to coincide, therefore we see that the diagonal entries of the state transition matrix are such that

$$\sum_{k=1}^{2n} S_{kk} = 0 \quad (25)$$

Note that the results in (23)-(25) hold for uniform and nonuniform structures, reciprocity provided.

## IV. SEGMENTATION TECHNIQUE

The general matricant approach in (9)-(11) is a superb numerical technique provided that the entries of the state-transition matrix $\mathbf{S}(x)$ are known in advance and are described by closed-form functions of $x$ —which seldom happens with real NUS.

However, sometimes, a discretized description of $\mathbf{S}$ may be available. The NUS, of length $l$, is conceptually broken down into a number $N$ of chained segments of length $\Delta l = l/N$, where each small segment, centered at $x = x_i = (2i-1)\Delta l/2$, is considered uniform. In other words, the $\mathbf{S}$ matrix is replaced by a stepwise approximation with $N$ steps, $\mathbf{S}_1 \ \cdots \ \mathbf{S}_N$, each small segment characterized by its transfer matrix, $\mathbf{T}_1 \ \cdots \ \mathbf{T}_N$,

$$\begin{cases} \mathbf{S}(x_1) = \mathbf{S}_1 \rightarrow \mathbf{T}_1 = e^{\mathbf{S}_1 \Delta l}, & \text{for } 0 < x < \Delta l \\ \quad \vdots \\ \mathbf{S}(x_N) = \mathbf{S}_N \rightarrow \mathbf{T}_N = e^{\mathbf{S}_N \Delta l}, & \text{for } l - \Delta l < x < l \end{cases} \quad (26)$$

The NUS transfer matrix is then obtained from

$$\mathbf{T}_l = \mathbf{T}_N \cdots \mathbf{T}_1 = e^{\mathbf{S}_N \Delta l} \ldots e^{\mathbf{S}_i \Delta l} \ldots e^{\mathbf{S}_1 \Delta l} \quad (27)$$

but, be aware, writing (27) in the form

$$\mathbf{T}_l = e^{\,\mathbf{S}_{av}\, l}, \quad \text{with } \mathbf{S}_{av} = \frac{1}{N}\sum_i \mathbf{S}_i \quad (28)$$

would be a mistake, for the multiplication of matrices is a non-commutative operation. Commutativity holds if all the $\mathbf{S}_i$ matrices share the same set of eigenvectors, [39], [40].

Nonetheless, an equivalent state transition matrix $\mathbf{S}_{eq}$ ($\neq \mathbf{S}_{av}$) based on the contributing $\mathbf{S}_i$ matrices can be defined

$$\mathbf{S}_{eq} = \tfrac{1}{N\Delta l} \ln\left(e^{\mathbf{S}_N \Delta l} \ldots e^{\mathbf{S}_i \Delta l} \ldots e^{\mathbf{S}_1 \Delta l}\right) \quad (29)$$

moreover, matrix $\mathbf{S}_{eq}$ can even be written in the form of a series expansion, like in (9)-(10).

The problem of finding the solution $\mathbf{S}_{eq}$ of the matrix equation

$$e^{\mathbf{S}_{eq}} = e^{\mathbf{S}_a} e^{\mathbf{S}_b} \quad (30)$$

in terms of known $\mathbf{S}_a$ and $\mathbf{S}_b$ is not a soft problem. During the 1900s, the problem was an issue of very great concern in the field of Physics (quantum mechanics/high energy) as well as in pure and applied Mathematics (linear algebra/Lie algebras). The so-called Baker-Campbell-Hausdorff-Dynkin formula, [42]–[48], provided a solution to (30) in the form of a series expansion with nested commutators whose first terms are

$$\begin{aligned} \mathbf{S}_{eq} = {} & (\mathbf{S}_a + \mathbf{S}_b) \\ & + \tfrac{1}{2!}[\mathbf{S}_a, \mathbf{S}_b] + \tfrac{2}{4!}[\mathbf{S}_a, [\mathbf{S}_a, \mathbf{S}_b]] + \tfrac{2}{4!}[\mathbf{S}_b, [\mathbf{S}_b, \mathbf{S}_a]] \cdots \end{aligned} \quad (31)$$

where the notation $[\mathbf{S}_a, \mathbf{S}_b]$ refers to the commutator of the $\mathbf{S}_a$ and $\mathbf{S}_b$ matrices, i.e., $[\mathbf{S}_a, \mathbf{S}_b] = \mathbf{S}_a\mathbf{S}_b - \mathbf{S}_b\mathbf{S}_a$.

It is now clear that the solution $\mathbf{S}_{eq} = \mathbf{S}_a + \mathbf{S}_b$, in (28), will only apply if $\mathbf{S}_a$ and $\mathbf{S}_b$ commute.

## V. TRANSFER MATRIX MEASUREMENT

Quite often, detailed data on the internal constitution of the NUS are badly known or unknown at all —the structure is a black box, accessible only at its input and output ends, $x = 0$ and $x = l$. In such circumstances, analytical tools are of little use to determine $\mathbf{T}_l$; the transfer matrix will have to be found experimentally, measuring the values of the state space complex phasors of the NUS gathered in the $n \times 1$ column matrices $\mathbf{P}_0$, $\mathbf{P}_l$, and $\mathbf{Q}_0$, $\mathbf{Q}_l$.

Let us go back to (2) and rewrite

$$\begin{bmatrix} \mathbf{P}_l \\ \mathbf{Q}_l \end{bmatrix} = \overbrace{\begin{bmatrix} \mathbf{A} & \mathbf{B} \\ \mathbf{C} & \mathbf{D} \end{bmatrix}}^{\mathbf{T}_l} \begin{bmatrix} \mathbf{P}_0 \\ \mathbf{Q}_0 \end{bmatrix} \quad (32)$$

By enforcing the boundary condition $\mathbf{Q}_0 = \mathbf{0}$ we have

$$\mathbf{P}_l = \mathbf{A}\mathbf{P}_0, \quad \mathbf{Q}_l = \mathbf{C}\mathbf{P}_0 \quad (33)$$

A first set of $n$ independent experiments is performed. In the $k^{\text{th}}$ experiment ($k = 1$ to $n$) the structure is driven at the output end by one single stimulus: $P_k(l) = p$ and $P_i(l) = 0$, for $i \neq k$. Afterward, the remaining state-space variables belonging to $\mathbf{P}_0$ and $\mathbf{Q}_l$ are measured.

Hence, we have:

Experiment #$k$ ($1^{\text{st}}$ set):

$$\mathbf{P}_l^{(k)} = p\begin{bmatrix} 0 \\ \vdots \\ 0 \\ 1 \\ 0 \\ \vdots \\ 0 \end{bmatrix} \rightarrow \mathbf{P}_0^{(k)} = \begin{bmatrix} P_1(0) \\ \vdots \\ P_{k-1}(0) \\ P_k(0) \\ P_{k+1}(0) \\ \vdots \\ P_n(0) \end{bmatrix}, \quad \mathbf{Q}_l^{(k)} = \begin{bmatrix} Q_1(l) \\ \vdots \\ Q_{k-1}(l) \\ Q_k(l) \\ Q_{k+1}(l) \\ \vdots \\ Q_n(l) \end{bmatrix} \quad (34)$$

The sets of $n$ stimuli and measurement results are separately gathered in three $n \times n$ square matrices

$$\begin{cases} \widehat{\mathbf{P}}_l = \left[\mathbf{P}_l^{(1)}, \cdots, \mathbf{P}_l^{(k)}, \cdots, \mathbf{P}_l^{(n)}\right] = p\mathbf{1} \\ \widehat{\mathbf{P}}_0 = \left[\mathbf{P}_0^{(1)}, \cdots, \mathbf{P}_0^{(k)}, \cdots, \mathbf{P}_0^{(n)}\right] \\ \widehat{\mathbf{Q}}_l = \left[\mathbf{Q}_l^{(1)}, \cdots, \mathbf{Q}_l^{(k)}, \cdots, \mathbf{Q}_l^{(n)}\right] \end{cases} \tag{35}$$

From (33) and (35) we see that submatrices $\mathbf{A}$ and $\mathbf{C}$ can be retrieved through

$$\mathbf{A} = p\widehat{\mathbf{P}}_0^{-1}, \quad \mathbf{C} = \widehat{\mathbf{Q}}_l\widehat{\mathbf{P}}_0^{-1} \tag{36}$$

Using a similar procedure the submatrices $\mathbf{B}$ and $\mathbf{D}$ are found from a new second set of $n$ experiments, where the boundary condition $\mathbf{P}_0 = \mathbf{0}$ is enforced, leading to

$$\mathbf{P}_l = \mathbf{B}\mathbf{Q}_0, \quad \mathbf{Q}_l = \mathbf{D}\mathbf{Q}_0 \tag{37}$$

As before, in the $k^{\text{th}}$ experiment ($k = 1$ to $n$) the structure is driven by the single stimulus $P_k(l) = p$, and the remaining state-space variables belonging to $\mathbf{Q}_0$ and $\mathbf{Q}_l$ are measured, that is:

Experiment #$k$ ($2^{\text{nd}}$ set):

$$\mathbf{P}_l^{(k)} = p\begin{bmatrix} 0 \\ \vdots \\ 0 \\ 1 \\ 0 \\ \vdots \\ 0 \end{bmatrix} \rightarrow \mathbf{Q}_0^{(k)} = \begin{bmatrix} Q_1(0) \\ \vdots \\ Q_{k-1}(0) \\ Q_k(0) \\ Q_{k+1}(0) \\ \vdots \\ Q_n(0) \end{bmatrix}, \quad \mathbf{Q}_l^{(k)} = \begin{bmatrix} Q_1(l) \\ \vdots \\ Q_{k-1}(l) \\ Q_k(l) \\ Q_{k+1}(l) \\ \vdots \\ Q_n(l) \end{bmatrix} \tag{38}$$

These measurements are gathered in two $n \times n$ square matrices $\breve{\mathbf{Q}}$

$$\begin{cases} \breve{\mathbf{Q}}_0 = \left[\mathbf{Q}_0^{(1)}, \cdots, \mathbf{Q}_0^{(k)}, \cdots, \mathbf{Q}_0^{(n)}\right] \\ \breve{\mathbf{Q}}_l = \left[\mathbf{Q}_l^{(1)}, \cdots, \mathbf{Q}_l^{(k)}, \cdots, \mathbf{Q}_l^{(n)}\right] \end{cases} \tag{39}$$

From (37) and (39) we see that submatrices $\mathbf{B}$ and $\mathbf{D}$ can be retrieved through

$$\mathbf{B} = p\breve{\mathbf{Q}}_0^{-1}, \quad \mathbf{D} = \breve{\mathbf{Q}}_l\breve{\mathbf{Q}}_0^{-1} \tag{40}$$

The correctness and precision of the measurements can be assessed/controlled by employing the transfer matrix properties in (12). From $\mathbf{A}^T\mathbf{C} = \mathbf{C}^T\mathbf{A}$ one must check that matrix $\widehat{\mathbf{Q}}_l$ is symmetric; likewise, from $\mathbf{D}^T\mathbf{B} = \mathbf{B}^T\mathbf{D}$ one must check the symmetry of $\breve{\mathbf{Q}}_l$. The remaining properties of the transfer matrix, listed in (12), may also be used to crosscheck the measurement data obtained in the two sets of experiments, which must be interdependent, provided, of course, that the structure under test suffered no internal changes during experiments.

The suggested sets of experiments —utilizing the same stimulus source in all the tests, where in each test only one output terminal of the NUS is excited— is just an example; many other options are equally possible.

Regardless of the option, careful attention should be paid to the need of synchronizing the measurements of the state-space complex phasors at the two ends of the NUS. Different delay times resulting from different distances between the measuring instrument and the two ends of the structure may corrupt the phase information.

The above aspect may not be of great concern when the measurement experiments are conducted on a lab bench. Things can get more complicated when the input and output ends of the NUS under test are some hundreds of miles apart, as it happens in the problem of real-time monitoring of overhead power lines —of undeniable socio-economic impact the problem is currently a hot topic of investigation, that involves synchrophasor measurement technology, phasor measurement units, smart grids, global positioning systems, and big data analytics, [50]–[52].

## VI. APPLICATION OF TRANSFER MATRIX METHOD TO NONUNIFORM MTL STRUCTURES

As was pointed out in the introductory section, the transfer matrix method (TMM) is a very important tool in electrical engineering for its utilization pervades a variety of areas, from long power lines operating at low frequency (60 Hz) to tiny optical devices functioning in the terahertz band.

Multiconductor transmission lines (MTL) is one of the most interesting cross-disciplinary subjects in electrical engineering and, for that reason, we chose it to exemplify the application of TMM to nonuniform structures.

An MTL structure is made of $n + 1$ electromagnetically coupled conductors (with $n \geq 2$), one of them named the reference or ground $0^{\text{th}}$ conductor. The MTL conductors, of length $l$, run longitudinally along the $x$-axis —see Fig. 1.

The state-space variables in (4) correspond here to the voltages $\mathbf{V}_x$ and currents $\mathbf{I}_x$ of the MTL conductors, that is

$$\boldsymbol{\Psi}(x) = \begin{bmatrix} \mathbf{P}_x \\ \mathbf{Q}_x \end{bmatrix} = \begin{bmatrix} \mathbf{V}_x \\ \mathbf{I}_x \end{bmatrix}, \quad \text{where: } \begin{cases} \mathbf{V}_x^T = \left[\bar{V}_1(x) \cdots \bar{V}_k(x) \cdots \bar{V}_n(x)\right] \\ \mathbf{I}_x^T = \left[\bar{I}_1(x) \cdots \bar{I}_k(x) \cdots \bar{I}_n(x)\right] \end{cases} \tag{41}$$

From MTL theory, [53]–[57], we have

$$\frac{d}{dx}\begin{bmatrix} \mathbf{V}_x \\ \mathbf{I}_x \end{bmatrix} = -\begin{bmatrix} \mathbf{0} & \mathbf{Z}_x \\ \mathbf{Y}_x & \mathbf{0} \end{bmatrix}\begin{bmatrix} \mathbf{V}_x \\ \mathbf{I}_x \end{bmatrix} \tag{42}$$

where $\mathbf{Z}_x = \mathbf{Z}(x, \omega)$ and $\mathbf{Y}_x = \mathbf{Y}(x, \omega)$ are, respectively, the per-unit-length impedance and admittance matrices of the MTL; both them are $n \times n$ nonsingular complex symmetric matrices, whose real and imaginary parts, if not null, are positive-definite.

From (6) and (42) we see the state transition matrix is such that

$$\mathbf{S}_x = -\begin{bmatrix} \mathbf{0} & \mathbf{Z}_x \\ \mathbf{Y}_x & \mathbf{0} \end{bmatrix}, \quad \begin{cases} \text{tr}(\mathbf{S}_x) = 0 \\ \det(\mathbf{S}_x) = (-1)^n \det(\mathbf{Z}_x\mathbf{Y}_x) \end{cases} \tag{43}$$

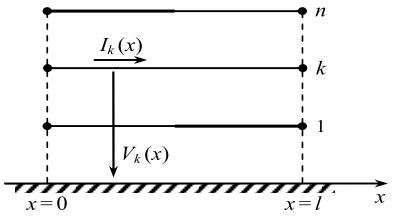


**FIGURE 1.** Voltages and currents along a nonuniform multiconductor transmission line with n+1 conductors of length l. Each conductor influences and is influenced by the remaining n conductors due to electromagnetic field coupling.

and

$$\begin{cases} \mathbf{S}_x^{2m} = \begin{bmatrix} \Gamma_x^{2m} & \mathbf{0} \\ \mathbf{0} & (\Gamma_x^{2m})^T \end{bmatrix} \\ \mathbf{S}_x^{2m+1} = -\begin{bmatrix} \mathbf{0} & \Gamma_x^{2m}\mathbf{Z}_x \\ \mathbf{Y}_x\Gamma_x^{2m} & \mathbf{0} \end{bmatrix} \end{cases} \tag{44}$$

where

$$\Gamma_x^2 = \mathbf{Z}_x\mathbf{Y}_x, \quad \Gamma_x^{2T} = \mathbf{Y}_x\mathbf{Z}_x \tag{45}$$

### A. MTL TRANSFER MATRIX

Next, we proceed to the determination of the transfer matrix $\mathbf{T}_l$ of the nonuniform MTL structure

$$\begin{bmatrix} \mathbf{V}_l \\ \mathbf{I}_l \end{bmatrix} = \overbrace{\begin{bmatrix} \mathbf{A} & \mathbf{B} \\ \mathbf{C} & \mathbf{D} \end{bmatrix}}^{\mathbf{T}_l} \begin{bmatrix} \mathbf{V}_0 \\ \mathbf{I}_0 \end{bmatrix} \tag{46}$$

employing the segmentation technique in Part IV, [58].

The NUS is broken down into $N$ chained uniform segments of length $l_i$ (with $l = \sum_{i=1}^{N} l_i$), each segment being described by discrete values of $\mathbf{Z}_i$ and $\mathbf{Y}_i$.

From (27) we have

$$\mathbf{T}_l = \mathbf{T}_N \cdots \mathbf{T}_i \cdots \mathbf{T}_1 = e^{\mathbf{S}_N l_N} \cdots e^{\mathbf{S}_i l_i} \cdots e^{\mathbf{S}_1 l_1} \tag{47}$$

where the exponential matrix $\mathbf{T}_i$ in (47) can be evaluated from the state transition matrix $\mathbf{S}_i$ using either the matricant approach or the diagonalization approach.

Using the matricant series expansion approach in (10) and (15), together with (44) leads to

$$\mathbf{T}_i = \begin{bmatrix} \mathbf{A}_i & \mathbf{B}_i \\ \mathbf{C}_i & \mathbf{D}_i \end{bmatrix} = e^{\mathbf{S}_i l_i} = \sum_{m=0}^{\infty} \frac{(\mathbf{S}_i l_i)^m}{m!}$$

$$= \sum_{m=0}^{\infty} \begin{bmatrix} \dfrac{(\Gamma_i l_i)^{2m}}{(2m)!} & -\dfrac{(\Gamma_i l_i)^{2m+1}}{(2m+1)!}(\Gamma_i^{-1}\mathbf{Z}_i) \\ -(\mathbf{Y}_i\Gamma_i^{-1})\dfrac{(\Gamma_i l_i)^{2m+1}}{(2m+1)!} & \dfrac{(\Gamma_i^T l_i)^{2m}}{(2m)!} \end{bmatrix} \tag{48}$$

or, in other words,

$$\begin{cases} \mathbf{A}_i = \mathbf{D}_i^T = \cosh(\Gamma_i l_i) \\ \mathbf{B}_i = \mathbf{B}_i^T = -\sinh(\Gamma_i l_i)\mathbf{Z}_B^{(i)} \\ \mathbf{C}_i = \mathbf{C}_i^T = -\mathbf{Y}_F^{(i)}\sinh(\Gamma_i l_i) \end{cases} \tag{49}$$

where $\mathbf{Y}_F^{(i)}$ and $\mathbf{Z}_B^{(i)}$, the so-called characteristic immittance matrices for forward and backward waves, respectively, are given by, [55], [59], [60],

$$\begin{cases} \mathbf{Y}_F^{(i)} = \mathbf{Y}_i\Gamma_i^{-1} \\ \mathbf{Z}_B^{(i)} = \Gamma_i^{-1}\mathbf{Z}_i \\ \text{with } \mathbf{Z}_B^{(i)}\mathbf{Y}_F^{(i)} = \Gamma_i^{-1}\mathbf{Z}_i\mathbf{Y}_i\Gamma_i^{-1} = \Gamma_i^{-1}\Gamma_i^2\Gamma_i^{-1} = \mathbf{1} \end{cases} \tag{50}$$

Since matrices $\mathbf{A}_i$, $\mathbf{B}_i$, $\mathbf{C}_i$, and $\mathbf{D}_i$ are already known for every MTL-segment $i = 1 \cdots N$, the global transfer matrix $\mathbf{T}_i$ can be evaluated using (47),

$$\mathbf{T}_l = \begin{bmatrix} \mathbf{A} & \mathbf{B} \\ \mathbf{C} & \mathbf{D} \end{bmatrix} = e^{\mathbf{S}_{eq} l} = \overbrace{\prod_{i=N}^{1} \left(e^{\mathbf{S}_i \Delta l}\right)}^{\mathbf{T}_i}$$

$$= \begin{bmatrix} \mathbf{A}_N & \mathbf{B}_N \\ \mathbf{C}_N & \mathbf{D}_N \end{bmatrix} \times \cdots \begin{bmatrix} \mathbf{A}_i & \mathbf{B}_i \\ \mathbf{C}_i & \mathbf{D}_i \end{bmatrix} \times \cdots \begin{bmatrix} \mathbf{A}_1 & \mathbf{B}_1 \\ \mathbf{C}_1 & \mathbf{D}_1 \end{bmatrix} \tag{51}$$

where the contributing matrices $\mathbf{T}_i$ and the final resulting matrix $\mathbf{T}_l$ have different properties, in general, $\mathbf{B}$ and $\mathbf{C}$ are not symmetrical and $\mathbf{D}$ is not the transposed of $\mathbf{A}$.

### B. MODAL ANALYSIS

MTLs are mainly used in EEE for transmission purposes (transmission of information or/and of energy) where the aspects of attenuation, delay time, load impedance matching, and so on, are of utmost concern.

To address these wave propagation aspects, well-known modal analysis techniques are used, [55]. The core idea is to find a vector-basis of $n$ independent uncoupled propagation modes, intrinsic to the MTL structure, onto which any propagation event can be projected, regardless of the complexity of its boundary conditions. This is accomplished through the diagonalization of the transfer matrix, as in (21), (22),

$$\mathbf{M}^{-1}\mathbf{T}_l\mathbf{M} = \begin{bmatrix} e^{-\gamma l} & \mathbf{0} \\ \mathbf{0} & e^{+\gamma l} \end{bmatrix} \tag{52}$$

where $\boldsymbol{\gamma}$ is a diagonal matrix, gathering the propagation constants $\gamma_1, \gamma_2, \cdots \gamma_n$ of the set of $n$ modes, conveying information about mode attenuation, phase, and velocity,

$$\text{Propagation constant: } \gamma_k = \alpha_k + j\beta_k, \quad \beta_k = \omega/v_k \tag{53}$$

By definition, a propagation mode is a peculiar fixed arrangement of voltages and currents that enforced at one end of the MTL will be replicated at the other end, multiplied by the scaling factor ($e^{\pm\gamma_k l}$), [55]–[57]. To account for wave reflection phenomena, each mode must include the contribution of two counter-propagating waves, the forward wave (along positive-$x$), and the backward wave (along negative-$x$).

The $2n \times 2n$ transformation matrix $\mathbf{M}$ in (52), whose columns $\mathbf{m}_1$ to $\mathbf{m}_{2n}$ are the eigenvectors of $\mathbf{T}_l$, can be block partitioned into four $n \times n$ submatrices,

$$\mathbf{M} = [\overbrace{\mathbf{m}_1, \cdots, \mathbf{m}_k, \cdots, \mathbf{m}_n}^{F-\text{wave}} \,|\, \overbrace{\mathbf{m}_{1+n}, \cdots, \mathbf{m}_{k+n}, \cdots, \mathbf{m}_{2n}}^{B-\text{wave}}]$$

$$= \begin{bmatrix} \mathbf{M}_{11} \,|\, \mathbf{M}_{12} \\ \mathbf{M}_{21} \,|\, \mathbf{M}_{22} \end{bmatrix} \tag{54}$$

where $\mathbf{M}_{11}$ and $\mathbf{M}_{22}$ are unitless, $\mathbf{M}_{12}$ is in $\Omega$, and $\mathbf{M}_{21}$ in $\Omega^{-1}$.

The eigenvectors $\mathbf{m}_k$ and $\mathbf{m}_{k+n}$ define the voltage and current arrangements of the forward and backward waves of the $k^{\text{th}}$ propagation mode, respectively. Hence, we should write,

$$\begin{cases} \begin{bmatrix} \mathbf{V}_l \\ \mathbf{I}_l \end{bmatrix}^{(F-\text{wave})}_{(\text{mode } k)} = e^{-\gamma_k l} \begin{bmatrix} \mathbf{V}_0 \\ \mathbf{I}_0 \end{bmatrix}^{(F-\text{wave})}_{(\text{mode } k)} \propto \mathbf{m}_k = \begin{bmatrix} \mathbf{M}_{11} \\ \mathbf{M}_{21} \end{bmatrix}_{(\text{column } k)} \\ \begin{bmatrix} \mathbf{V}_l \\ \mathbf{I}_l \end{bmatrix}^{(B-\text{wave})}_{(\text{mode } k)} = e^{+\gamma_k l} \begin{bmatrix} \mathbf{V}_0 \\ \mathbf{I}_0 \end{bmatrix}^{(B-\text{wave})}_{(\text{mode } k)} \propto \mathbf{m}_{k+n} = \begin{bmatrix} \mathbf{M}_{12} \\ \mathbf{M}_{22} \end{bmatrix}_{(\text{column } k)} \end{cases} \tag{55}$$

$$\begin{cases} \begin{Bmatrix} \mathbf{I}_l^{(F-\text{wave})} \\ \mathbf{I}_0^{(F-\text{wave})} \end{Bmatrix} = +\mathbf{Y}_F \begin{Bmatrix} \mathbf{V}_l^{(F-\text{wave})} \\ \mathbf{V}_0^{(F-\text{wave})} \end{Bmatrix}, \ \mathbf{Y}_F = +\mathbf{M}_{21}\mathbf{M}_{11}^{-1} \\ \begin{Bmatrix} \mathbf{V}_l^{(B-\text{wave})} \\ \mathbf{V}_0^{(B-\text{wave})} \end{Bmatrix} = -\mathbf{Z}_B \begin{Bmatrix} \mathbf{I}_l^{(B-\text{wave})} \\ \mathbf{I}_0^{(B-\text{wave})} \end{Bmatrix}, \ \mathbf{Z}_B = -\mathbf{M}_{12}\mathbf{M}_{22}^{-1} \end{cases} \tag{56}$$

In the general case of nonuniform MTLs, the forward characteristic admittance matrix $\mathbf{Y}_F$, and the backward characteristic impedance matrix $\mathbf{Z}_B$ are not inverse of each other. The $2n$-order diagonalization problem in (52)

$$\begin{bmatrix} \mathbf{A} & \mathbf{B} \\ \mathbf{C} & \mathbf{D} \end{bmatrix} \begin{bmatrix} \mathbf{M}_{11} & \mathbf{M}_{12} \\ \mathbf{M}_{21} & \mathbf{M}_{22} \end{bmatrix} = \begin{bmatrix} \mathbf{M}_{11} & \mathbf{M}_{12} \\ \mathbf{M}_{21} & \mathbf{M}_{22} \end{bmatrix} \begin{bmatrix} e^{-\gamma l} & \mathbf{0} \\ \mathbf{0} & e^{+\gamma l} \end{bmatrix} \tag{57}$$

has to be solved as a whole —the problem does not split into two independent $n$-order diagonalization sub-problems.

This is possible in one case only: when the NUS is longitudinally symmetric, i.e., when the input and output ends of the MTL are indiscernible, interchangeable. In this case, the properties of $\mathbf{A}$, $\mathbf{B}$, $\mathbf{C}$, $\mathbf{D}$ in (17) can be used, and from (57) and (17) we find,

$$\begin{cases} \mathbf{M}_{11}^{-1} = \mathbf{M}_{22}^{T}, \quad \mathbf{M}_{21}^{-1} = -\mathbf{M}_{12}^{T} \\ \mathbf{M}_{11}^{-1}\mathbf{A}\mathbf{M}_{11} = \mathbf{M}_{22}^{-1}\mathbf{D}\mathbf{M}_{22} = \cosh(\gamma l) \\ \mathbf{M}_{11}\mathbf{M}_{21}^{-1} = -\mathbf{M}_{12}\mathbf{M}_{22}^{-1} \ \rightarrow \ \mathbf{Y}_F\mathbf{Z}_B = \mathbf{1} \end{cases} \tag{58}$$

showing, not only, how the set of $n$ modal propagation constants can be obtained, but also, that the characteristic immittance matrices for forward and backward propagation coincide. The symmetrical characteristic admittance matrix $\mathbf{Y}_w$ necessary for load matching at both ends of the MTL, is obtained from (55)-(58). Taking into account that, for longitudinally symmetric NUS, matrices $\mathbf{B}$ and $\mathbf{C}$ are both symmetrical, the equation for the computation of $\mathbf{Y}_w$ may be written in various formats:

$$\mathbf{Y}_w = \mathbf{Y}_F = \mathbf{Z}_B^{-1} = \begin{cases} \mathbf{B}^{-1}(\mathbf{B}\mathbf{C})^{1/2} = (\mathbf{C}\mathbf{B})^{1/2}\mathbf{B}^{-1} \\ \mathbf{C}\,(\mathbf{B}\mathbf{C})^{-1/2} = (\mathbf{C}\mathbf{B})^{-1/2}\mathbf{C} \end{cases} \tag{59}$$

where

$$\begin{Bmatrix} \mathbf{B}\mathbf{C} \\ \mathbf{C}\mathbf{B} \end{Bmatrix} = \begin{Bmatrix} \mathbf{M}_{11} \\ \mathbf{M}_{22} \end{Bmatrix} \sinh^2(\gamma l) \begin{Bmatrix} \mathbf{M}_{11}^{-1} \\ \mathbf{M}_{22}^{-1} \end{Bmatrix} \tag{60}$$

As a parenthetical note, we may add that the basic case of uniform MTLs —see (48)-(50)— is a subcase of (58), where the $n \times n$ transformation matrix $\mathbf{M}_{11}$ brings the product matrix $\mathbf{Z}\mathbf{Y}$ $(= \Gamma^2)$ to diagonal form:$\mathbf{M}_{11}^{-1}\Gamma\mathbf{M}_{11} = \gamma$.

### C. EXEMPLIFICATION AND NOVEL RESULTS

The present review dedicated to the transfer matrix method theory and its applications to nonuniform structures is now complemented with a novel research contribution to the field of NUS/MTL.

In a recent IEEE Transactions paper [61] the authors managed to prove theoretically that longitudinally asymmetric nonuniform MTLs (where $\mathbf{D} \neq \mathbf{A}^T$ ) could, in special circumstances, require the presence of negative load resistors to ensure full matching conditions; load matching is feasible for each and every individual mode, but may not be when modes coexist.

On the other hand, load matching is always physically possible for any uniform MTL, where $\mathbf{D} = \mathbf{A}^T$.

The pending issue is: What if the MTL is nonuniform but longitudinally symmetric? May negative resistors still be needed for full load matching?

The issue is addressed here using the analytical tools in parts A and B. The simple structure ($n = 2$) shown in Fig. 2 is used for exemplification purposes. The example describes the chain connection of two equal, bilaterally symmetric, uniform stripline couplers of length $l/2$. The structure's nonuniformity is created by a perturbation, occurring at the junction's plane, modeled through the lumped impedances $Z_J$.

To simplify matters, we will consider the usual high-frequency approximation $\alpha/\beta \rightarrow 0$, tantamount to saying that the couplers are lossless, with purely real characteristic wave admittances.

The transfer matrix of the NUS is obtained from (51)

$$\begin{aligned} \mathbf{T}_l = \begin{bmatrix} \mathbf{A} & \mathbf{B} \\ \mathbf{C} & \mathbf{D} \end{bmatrix} = e^{\mathbf{S}_{eq.}\, l} = \prod_{i=3}^{1} \begin{bmatrix} \mathbf{A}_i & \mathbf{B}_i \\ \mathbf{C}_i & \mathbf{D}_i \end{bmatrix} \\ = \mathbf{T}_3\mathbf{T}_2\mathbf{T}_1 = \mathbf{T}\mathbf{T}_J\mathbf{T} \end{aligned} \tag{61}$$

where $\mathbf{T} = \mathbf{T}_1 = \mathbf{T}_3$ is the transfer matrix of each stripline coupler of length $l/2$. Owing to couplers' bilateral symmetry, the $2 \times 2$ submatrices $\mathbf{A}_1$, $\mathbf{B}_1$, $\mathbf{C}_1$, and $\mathbf{D}_1$, are not only symmetric but also have the same diagonal entries, which makes them similar matrices, commutable matrices, sharing the same set of eigenvectors,

$$\begin{aligned} \mathbf{M}_{11} &= \mathbf{M}_{22} = [\mathbf{m}_1\ \mathbf{m}_2], \\ \mathbf{m}_1 &= \tfrac{1}{\sqrt{2}} \begin{bmatrix} 1 \\ 1 \end{bmatrix} \text{ and } \mathbf{m}_2 = \tfrac{1}{\sqrt{2}} \begin{bmatrix} 1 \\ -1 \end{bmatrix} \end{aligned} \tag{62}$$

Note that the eigenvectors $\mathbf{m}_1$ and $\mathbf{m}_2$ define the familiar pair of even & odd modes, the transformation matrices $\mathbf{M}_{ii}$ being symmetric and orthogonal,

$$\mathbf{M}_{ii} = \mathbf{M}_{ii}^{-1} = \mathbf{M}_{ii}^{T} = \tfrac{1}{\sqrt{2}} \begin{bmatrix} 1 & 1 \\ 1 & -1 \end{bmatrix}, \quad i = 1, 2 \tag{63}$$

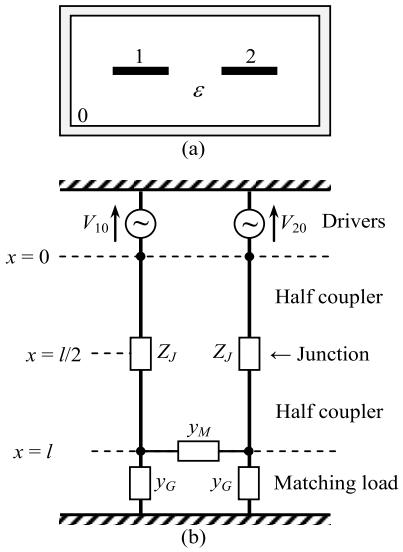


**FIGURE 2.** Symmetric nonuniform MTL structure. (a) Couplers' cross-section. (b) Longitudinal view showing the perturbation at the junction's plane (x = l/2), and the network of matching load admittances (x = l).

From (45), (48)-(50), and (58)-(60), we obtain

$$\begin{cases} \mathbf{A}_1 = \mathbf{D}_1 = \mathbf{A}_3 = \mathbf{D}_3 = \left(\cosh\frac{\gamma l}{2}\right)\mathbf{1} \\ \mathbf{B}_1 = \mathbf{B}_3 = -\left(\sinh\frac{\gamma l}{2}\right)\mathbf{Y}_u^{-1} \\ \mathbf{C}_1 = \mathbf{C}_3 = -\left(\sinh\frac{\gamma l}{2}\right)\mathbf{Y}_u \end{cases} \tag{64}$$

and

$$\mathbf{Y}_u = \mathbf{Y}_w^{(1\text{ or }3)} = \begin{cases} \mathbf{Y}_1\Gamma_1^{-1} = \left(j\omega c_{11}\begin{bmatrix} 1 & -k \\ -k & 1 \end{bmatrix}\right)\left(\frac{1}{\gamma}\begin{bmatrix} 1 & 0 \\ 0 & 1 \end{bmatrix}\right) \\ vc_{11}\begin{bmatrix} 1 & -k \\ -k & 1 \end{bmatrix} = \mathbf{M}_{11}\begin{bmatrix} Y_e & 0 \\ 0 & Y_o \end{bmatrix}\mathbf{M}_{11}^{-1} \end{cases} \tag{65}$$

where:

- $\gamma = j\beta = j\omega/v$ is the imaginary propagation constant of traveling waves in a nonmagnetic lossless medium with velocity $v = (\mu_0\varepsilon)^{-1/2}$ where $\varepsilon$ is the permittivity of the couplers' dielectric medium (Fig. 2a).
- $\mathbf{Y}_u$ is the $n \times n$ characteristic admittance matrix of both uniform couplers 1 and 3.
- $k$ is the strips' coupling factor,

$$k = \sqrt{\frac{c_{12}c_{21}}{c_{11}c_{22}}} = \frac{|c_{12}|}{c_{11}}, \quad 0 < k < 1 \tag{66}$$

where $c_{11} = c_{22}$ ( $> 0$) and $c_{12} = c_{21}$ ($< 0$) are the entries of the per-unit-length capacitance matrix of the uniform stripline couplers.

- $Y_e$ and $Y_o$ are the scalar characteristic admittances of the even and odd modes of the uniform couplers, respectively,

$$Y_e = \frac{G}{1+k}, \quad Y_o = \frac{G}{1-k}, \; Y_e < Y_o \tag{67}$$

where $G$ is the characteristic wave conductance of the same stripline coupler but with one single strip.

Observing the couplers' junction (Fig. 2b) readily leads to the junction's transfer matrix $\mathbf{T}_J = \mathbf{T}_2$,

$$\mathbf{T}_J = \begin{cases} \begin{bmatrix} \mathbf{A}_J & \mathbf{B}_J \\ \mathbf{C}_J & \mathbf{D}_J \end{bmatrix}, & \text{where } \begin{cases} \mathbf{A}_J = \mathbf{D}_J = \mathbf{1} \\ \mathbf{B}_J = -Z_J\mathbf{1}, \; \mathbf{C}_J = \mathbf{0} \end{cases} \\ \mathbf{1} + Z_J\mathbf{U}, & \text{where } \mathbf{U} = \begin{bmatrix} \mathbf{0} & -\mathbf{1} \\ \mathbf{0} & \mathbf{0} \end{bmatrix} \end{cases} \tag{68}$$

Now, with the help of (61), (64), and (68), we get the global NUS' transfer matrix:

$$\mathbf{T}_l = \begin{bmatrix} \mathbf{A} & \mathbf{B} \\ \mathbf{C} & \mathbf{D} \end{bmatrix} = \mathbf{T}\mathbf{T}_J\mathbf{T} = \mathbf{T}^2 + \overbrace{(Z_J\mathbf{T}\mathbf{U}\mathbf{T})}^{\mathbf{P}} \tag{69}$$

where the unperturbed term $\mathbf{T}^2$ describes a uniform stripline coupler of length $l$, that is

$$\mathbf{T}^2 = \begin{cases} \begin{bmatrix} \mathbf{A}_1^2 + \mathbf{B}_1\mathbf{C}_1 & 2\mathbf{A}_1\mathbf{B}_1 \\ 2\mathbf{A}_1\mathbf{C}_1 & \mathbf{A}_1^2 + \mathbf{B}_1\mathbf{C}_1 \end{bmatrix} \\ \begin{bmatrix} \cosh\gamma l\,\mathbf{1} & -\sinh\gamma l\,\mathbf{Y}_u^{-1} \\ -\sinh\gamma l\,\mathbf{Y}_u & \cosh\gamma l\,\mathbf{1} \end{bmatrix} \end{cases} \tag{70}$$

while the junction's perturbation term $\mathbf{P}$ is

$$\mathbf{P} = Z_J \times \begin{cases} -\begin{bmatrix} \mathbf{A}_1\mathbf{C}_1 & \mathbf{A}_1^2 \\ \mathbf{C}_1^2 & \mathbf{A}_1\mathbf{C}_1 \end{bmatrix} \\ \begin{bmatrix} \frac{1}{2}\sinh\gamma l\,\mathbf{Y}_u & -\cosh^2(\frac{\gamma l}{2})\,\mathbf{1} \\ -\sinh^2(\frac{\gamma l}{2})\,\mathbf{Y}_u^2 & \frac{1}{2}\sinh\gamma l\,\mathbf{Y}_u \end{bmatrix} \end{cases} \tag{71}$$

Then, from (69)-(71), we find the submatrices $\mathbf{A}$, $\mathbf{B}$, $\mathbf{C}$, and $\mathbf{D}$ belonging to the global transfer matrix $\mathbf{T}_l$

$$\begin{cases} \mathbf{A} = \mathbf{A}^T = \mathbf{D} = \left(\cosh\gamma l\,\mathbf{1} + \frac{1}{2}Z_J\mathbf{Y}_u\,\sinh\gamma l\right) \\ \mathbf{B} = \mathbf{B}^T = -\left(\sinh\gamma l\,\mathbf{1} + Z_J\mathbf{Y}_u\cosh^2(\frac{\gamma l}{2})\right)\mathbf{Y}_u^{-1} \\ \mathbf{C} = \mathbf{C}^T = -\mathbf{Y}_u\left(\sinh\gamma l\,\mathbf{1} + Z_J\mathbf{Y}_u\sinh^2(\frac{\gamma l}{2})\right) \end{cases} \tag{72}$$

The above submatrices are symmetric, commute, and are diagonalizable by the transformation matrix $\mathbf{M}_{11}$ in (63). Owing to this feature, the computation of the characteristic admittance matrix of the NUS, (59), greatly simplifies, yielding

$$\begin{aligned} \mathbf{Y}_w = \mathbf{C}^{1/2}\mathbf{B}^{-1/2} &= \mathbf{M}_{11}\begin{bmatrix} y_e & 0 \\ 0 & y_o \end{bmatrix}\mathbf{M}_{11}^{-1} \\ &= \frac{1}{2}\begin{bmatrix} y_e + y_o & y_e - y_o \\ y_e - y_o & y_e + y_o \end{bmatrix} \\ &= \underbrace{(y_e)}_{y_G}\mathbf{1} + \underbrace{\tfrac{1}{2}(y_o - y_e)}_{y_M}\begin{bmatrix} 1 & -1 \\ -1 & 1 \end{bmatrix} \end{aligned} \tag{73}$$

where the parameters $y_G = g_G + js_G$ and $y_M = g_M + js_M$ are, respectively, the strip-to-ground admittance and the mutual (interstrip) admittance that characterize the matched

load network at $x = l$ in Fig. 2b, where $y_m$ (for $m = e,\ o$) is given by,

$$y_m = \sqrt{\frac{C_m}{B_m}} = Y_m \sqrt{\frac{\sinh \gamma l + Z_J Y_m \sinh^2(\frac{\gamma l}{2})}{\sinh \gamma l + Z_J Y_m \cosh^2(\frac{\gamma l}{2})}} \tag{74}$$

If the perturbation **P** were absent ($Z_J = 0$) we would get, from (73), (74), (65), and (67),

$$\lim_{Z_J \to 0} \mathbf{Y}_w = \mathbf{M}_{11} \begin{bmatrix} Y_e & 0 \\ 0 & Y_o \end{bmatrix} \mathbf{M}_{11}^{-1} = \mathbf{Y}_u \tag{75}$$

$$\lim_{Z_J \to 0} \begin{Bmatrix} y_G \\ y_M \end{Bmatrix} = \frac{G}{1-k^2} \begin{Bmatrix} 1-k \\ k \end{Bmatrix} > 0 \tag{76}$$

Recent research on the subject of NUS, [60], [61], has shown that the issue of load matching realizability is worthy of attention only when the NUS resonates, when its length $l$ approaches a multiple of a one-half wavelength. Here, we will focus on the first resonance event, $l \approx \lambda/2$, $\beta l \approx \pi$, $\omega \approx \omega_{res} = v\pi/l$ and, for exemplification, consider the case of a capacitive junction's perturbation $Z_J$

$$Z_J(\omega) = \frac{1}{j\omega C_J}, \quad Z_J(\omega_{res}) = -jX_{res} \tag{77}$$

One may imagine that the junction's perturbation is originated by a manufacturing defect that prevents the left and right halves of the coupler to fully connect owing to an unintended tiny gap between the contacting ends of the strips.

By making

$$\gamma l = j\beta l = j(\pi + \theta),\ \theta = \pi \left( \frac{\omega - \omega_{res}}{\omega_{res}} \right) \tag{78}$$

we can rewrite (74) as

$$y_m = Y_m \sqrt{\frac{\omega C_J \sin\theta - Y_m \cos^2(\frac{\theta}{2})}{\omega C_J \sin\theta + Y_m \sin^2(\frac{\theta}{2})}} \tag{79}$$

For the case of small perturbations, $\omega_{res} C_J \ll Y_m$, $\theta \ll \pi$, the above result simplifies to

$$\begin{cases} y_m(\theta) = Y_m \underbrace{\sqrt{|1 - \vartheta_m|}}_{h_m(\theta) \geq 0} \times \begin{cases} -j, \text{ for } \vartheta_m > 1 \\ 1, \text{ otherwise} \end{cases} \\ \text{where } \vartheta_m(\theta) = Y_m X_{res} \left( \dfrac{1}{\theta} - \dfrac{1}{\pi} \right) \end{cases} \tag{80}$$

which leads to the following conclusions

a) The frequency-dependent characteristic admittances $y_m$ of the NUS' propagation modes cannot exhibit negative real part, regardless of the frequency;

b) At resonance, $\theta = 0$, one gets $y_m \to \infty$, meaning that the matched load is a full short-circuit termination;

c) For $\vartheta_m > 1$, the characteristic admittance $y_m$ of the $m$-mode is purely imaginary —the modes' active power at the MTL ends is zero; electromagnetic waves are pure standing waves, the NUS behaves as a stopband filter.

Also from (80), and (73), we learn that:

d) The strip-to-ground load admittance required for MTL matching can never exhibit negative real part, $g_G = \Re(y_G) = \Re(y_e) \geq 0$ ;

e) The real part of the mutual (interstrip) admittance required for MTL matching, $g_M = \Re(y_M) = \Re(y_o - y_e)/2$, can be negative, turning the load network in Fig. 2b into a physically non-realizable termination.

At this point it is convenient to introduce a set of three critical frequency values:

— the cutoff frequency $\omega = \omega_e$ (or $\theta = \theta_e$), for which the $e$-mode transitions from stop to pass-band behavior.

— the cutoff frequency $\omega = \omega_o$ (or $\theta = \theta_o$), for which the $o$-mode transitions from stop to pass-band behavior.

— the crossover frequency $\omega = \omega_x$ (or $\theta = \theta_x$), for which the real positive characteristic admittance $\omega-$functions cross each other, $y_e(\omega_x) = y_o(\omega_x)$.

After some algebra we find

$$\theta_m = X_{res} Y_m - \frac{(X_{res} Y_m)^2}{\pi}, \quad \text{for } m = e,\ o,\ x \tag{81}$$

where $Y_e$ and $Y_o$ are defined in (67) and $Y_x$ is obtained from them through

$$Y_x = Y_e + Y_o - \frac{Y_e Y_o}{Y_e + Y_o} = \frac{G}{2} \left( \frac{3 + k^2}{1 - k^2} \right) \tag{82}$$

The terms $(X_{res} Y_m)^2$ in (81) are $2^{\text{nd}}$ order corrections due to small variations of the junction's impedance near to resonance. For the sake of simplicity, those corrections will be disregarded. The results that follow are accurate only at first-order approximation level.

The case of a nonrealizable matched load ($g_M < 0$) occurs in the narrow band $\theta \in [\theta_e,\ \theta_x]$ whose width $\Delta\theta$ is

$$\Delta\theta = \theta_x - \theta_e = \frac{G}{2} \left( \frac{1+k}{1-k} \right) X_{res} \tag{83}$$

In the interval $[\theta_e,\ \theta_o]$ the $o$-mode is inside its stopband, but the $e$-mode is out. From (80) we get

$$y_M(\theta) = g_M + j s_M = -\frac{G}{2} \left( \frac{h_e(\theta)}{1+k} - j \frac{h_o(\theta)}{1-k} \right) \tag{84}$$

In the interval $[\theta_o,\ \theta_x]$ both modes are outside their stopbands. From (80) we get

$$y_M(\theta) = g_M = -\frac{G}{2} \left( \frac{h_e(\theta)}{1+k} - \frac{h_o(\theta)}{1-k} \right) + j0 \tag{85}$$

For $\theta = \theta_e$ and $\theta = \theta_x$ the interstrip conductance $g_M$ is zero. For $\theta = \theta_o$ it reaches its negative peak value:

$$g_M^{\min}(k) = -\tfrac{1}{2} y_e = -G \sqrt{\frac{k}{2(1+k)^3}} \tag{86}$$

The peak value is zero for uncoupled strips, increases up to its extremal value $(g_M^{\min})_{\max} = -G(2/3^3)^{1/2}$ at $k = 1/2$, and decreases afterward.

Albeit a first-order approximation, the above results are remarkable. They reveal two interesting things about the

negative peak value of the interstrip matching conductance. Firstly: It barely depends on the junction's reactance $X_{res}$ and, secondly, it cannot exceed a certain limit.

The apparently paradoxical assertion that the peak value $g_M^{\min}$ barely depends on the junction's reactance must be read from a distance. Consider a uniform coupler ($Z_J = 0$); how come can it require a negative interstrip conductance for matching purposes? It cannot. The point is that the relevance of negatively valued $g_M(\omega)$ must not be assessed by simply looking at its peak value. As shown in (83) the spectral width $\Delta\theta$ of the "$g_M < 0$ phenomenon" is directly proportional to the junction's reactance perturbation. When $X_{res}$ goes to zero, $\theta_e$, $\theta_o$ and $\theta_x$ will go with it ($\omega_x = \omega_o = \omega_e = \omega_{res}$), i.e., the negative part of the $g_M(\omega)$ function has no $\omega-$support, the phenomenon is inexistent for $Z_J = 0$.

Numerical and simulation results are presented next, the following realistic data being considered:

$$k = \frac{1}{2}, \quad G = \frac{1}{50\ \Omega} \quad \rightarrow \quad Y_e = \frac{Y_o}{3} = \frac{1}{75\ \Omega} \tag{87}$$

The corresponding array of matching load resistances for the uniform MTL coupler is depicted in Fig. 3a; the strip-to-ground load and the interstrip load are equal to 75 Ω, both positive of course.

With regard to the junction's capacitive perturbation, we take

$$GX_{res} = 0.1 \rightarrow X_{res} = 5\ \Omega \tag{88}$$

Using the data in (87)-(88) we run MATLAB to compute the normalized matching load admittances $y_G(\omega)/G$ and $y_M(\omega)/G$ directly from the core equations (72)-(73) and (77), without simplifications. Numerical simulation results for the half-wavelength resonance case are offered in Fig. 4 and Fig. 5, where the horizontal axis is the normalized frequency ($\omega/\omega_{res}$) varying in the vicinity of 1, in a narrow frequency band where $\omega_{res}$, $\omega_e$, $\omega_o$, and $\omega_x$ are included.

Fig. 4 and Fig. 5 depict the real and imaginary parts of the strip-to-ground load admittance $y_G$ (dashed lines) and the interstrip load admittance $y_M$ (solid lines). Fig. 4 concerns the normalized conductance functions $g_G/G$ and $g_M/G$ while Fig. 5 concerns the normalized susceptance functions $s_G/G$ and $s_M/G$. The circle marks sequentially identify, from left to right, the notable frequencies $\omega_{res}$, $\omega_e$, $\omega_o$, and $\omega_x$, respectively.

Fig. 3b shows the resistors' array (with $r = g_M^{-1}$) needed to load matching the NUS MTL-coupler at $\omega = \omega_o$, when $g_M$ reaches its negative peak value. Rest assured that the presence of the negative resistor in Fig. 3b does not violate any physical principle. No matter the enforced set of voltages, the power delivered to the load can never be negative: $p_{load} = \frac{1}{r}(V_1 + V_2)^2 \geq 0$.

For verification purposes, the exact MATLAB numerical results were checked against the analytical first-order approximate results in (81)-(86): the agreement is quite good —see Table 1.

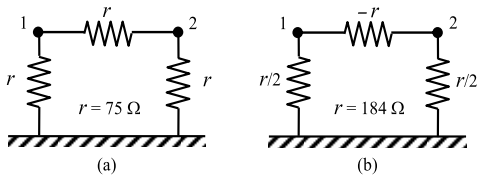


**FIGURE 3.** Array of lumped load resistors required for a matched termination of the MTL-coupler. (a) Unperturbed coupler case, $Z_J = 0$; frequency-independent matching. b) Perturbed coupler case, $Z_J(\omega) = -jX$, $X(\omega_{res}) = 5\Omega$; matching at $\omega = \omega_o$, when $g_M$ reaches its negative peak.

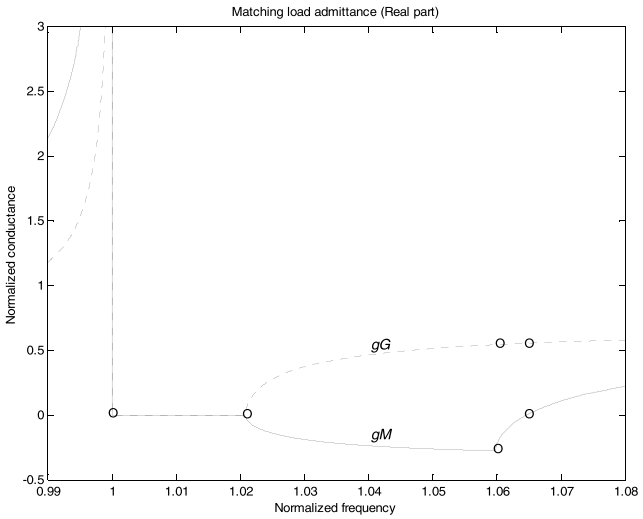


**FIGURE 4.** Normalized conductance functions $g_G$ and $g_M$ against $\omega/\omega_{res}$. Frequency plots of the real part of the strip-to-ground (dashed curve) and interstrip (solid curve) matching load admittances of the MTL coupler perturbed at the junction's plane by insertion of a capacitive impedance of –j5Ω.

Fig. 6 is, in part, a zooming in Fig. 4. It highlights the details of the frequency-dependent normalized interstrip matched-load conductance $g_M(\omega)$, focusing on the $\omega-$band where $g_M$ is a negatively valued function.

Curve (a) is an amplified replica of the solid line in Fig. 4, for the case $Z_J = -jX_{res}\omega_{res}/\omega$, with $X_{res} = 5\ \Omega$.

The dashed curve (b) was obtained by considering that the junction's impedance perturbation, in addition to its reactive part, also includes a resistive part $R_J$. Here, for $\omega = \omega_{res}$, we will take $Z_J = (\delta - j)\, X_{res}$, with $X_{res} = 5\ \Omega$ and $\delta = 5\%$. As shown in Fig. 6 the evolution of $g_M(\omega)$ through negative values is still present, leading again to a non-realizable matching load despite the presence of losses at the coupler's junction. The main effect of $R_J$ is to smooth out the sharp corners in curve (a), at the critical frequencies $\omega_e$ and $\omega_o$.

Curve (c), in blue, illustrates the interesting results in (86) and (83), considering the case $Z_J = -jX_{res}\,\omega_{res}/\omega$ with $X_{res} = 2.5\ \Omega$. The capacitive junction's perturbation was decreased 50% with respect to curve (a). One can see that the bandwidth of the "$g_M < 0$ phenomenon" has also squeezed 50% but the negative peak value of $g_M$ remained practically unaltered, $g_M(\omega_o) = -0.272G$.

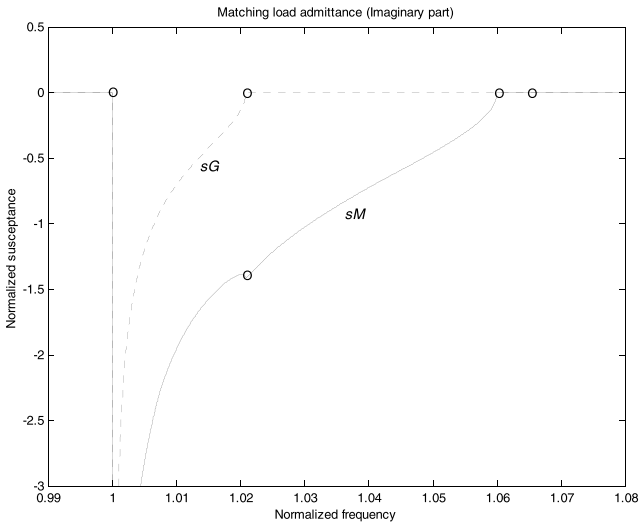


**FIGURE 5.** Normalized susceptance functions $s_C$ and $s_M$ against $\omega/\omega_{res}$. Frequency plots of the imaginary part of the strip-to-ground (dashed curve) and interstrip (solid curve) matching load admittances of the MTL coupler perturbed at the junction's plane by insertion of a capacitive impedance of –j5Ω.

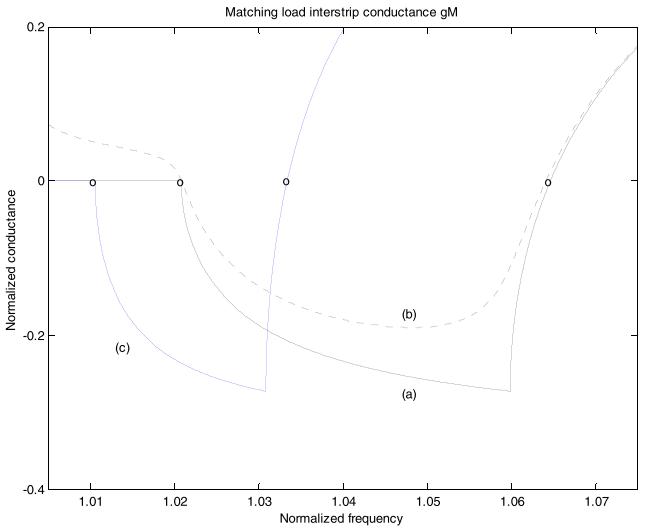


**FIGURE 6.** Frequency plots of the real part of the normalized interstrip matching load admittance $g_M$ of the MTL-coupler perturbed at the junction's plane by insertion of an impedance $Z_J = R_J - jX$ whose assigned value (at $\omega_{res}$) is as indicated: Curve (a): $X = 5\Omega$ and $R_J = 0$. Curve (b): $X = 5\Omega$ and $R_J = X/20$. Curve (c): $X = 2.5\Omega$ and $R_J = 0$. Leftmost circle marks correspond to $\omega_e$, rightmost to $\omega_x$.

**TABLE 1.** Wave parameters of the NUS MTL-Coupler at resonance.

| Quantity (normalized) | MATLAB, numerical (72)-(73) | 1st order analytical (81)-(86) |
|---|---|---|
| $\omega_e/\omega_{res}$ | 1.0208 | 1.0212 |
| $\omega_o/\omega_{res}$ | 1.0600 | 1.0637 |
| $\omega_x/\omega_{res}$ | 1.0646 | 1.0690 |
| $(\omega_x-\omega_e)/\omega_{res}$ | 0.0438 | 0.0477 |
| $g_M^{\min}/G$ | –0.2718 | –0.2722 |
| $\omega=\omega_e: \begin{cases} y_G/G \\ y_M/G \end{cases}$ | 0<br>–j1.4118 | 0<br>–j1.4138 |
| $\omega=\omega_o: \begin{cases} y_G/G \\ y_M/G \end{cases}$ | 0.5435<br>-0.2718 | 0.5443<br>–0.2722 |
| $\omega=\omega_x: \begin{cases} y_G/G \\ y_M/G \end{cases}$ | 0.5539<br>0 | 0.5547<br>0 |

## VII. CONCLUSION

This article was devoted to the transfer matrix method largely utilized in a variety of electrical engineering areas, from power systems to optics, as well as in other science fields, from materials to DNA research.

As the name suggests, the method is aimed to transfer information/data from one system's boundary end to another boundary end, using conversion rules dictated by the internal constitution of the system. Reciprocally, the system's properties can be retrieved from measurements at its ends.

The above aspects were dealt with in Sections II to V, offering the reader a survey on the formalisms adequate for the analysis of general *n*-port nonuniform systems (NUS), including the matricant or state-space approach, the diagonalization or modal-analysis approach, and also the segmentation technique.

The article's longest section —the sixth— focused on the concrete case of multiconductor transmission-line systems (MTL) which are of great importance to electrical engineers involved in guided-wave propagation problems. MTL equations and general transfer matrix solutions were reviewed and, in addition, an interesting novel research result was delivered; we succeeded to prove that a very simple two-port NUS, longitudinally and transversally symmetric, lossless or lossy, cannot always be terminated on a realizable matched load.

## REFERENCES

[1] L. Brillouin, *Wave Propagation in Periodic Structures*. New York, NY, USA: Dover, 1946.
[2] H. Matsuda, "The transfer matrix method in the theory of normal vibrations of chain molecules," *Prog. Theor. Phys.*, vol. 23, pp. 22–58, Mar. 1962.
[3] A. Kumar and T. Sankar, "A new transfer matrix method for response analysis of large dynamic systems," *Comput. Struct.*, vol. 23, no. 4, pp. 545–552, Jan. 1986.
[4] B. Stout, J.-C. Auger, and J. Lafait, "A transfer matrix approach to local field calculations in multiple-scattering problems," *J. Mod. Opt.*, vol. 49, no. 13, pp. 2129–2152, Nov. 2002.
[5] L.-L. Lin, Z.-Y. Li, and K.-M. Ho, "Lattice symmetry applied in transfer-matrix methods for photonic crystals," *J. Appl. Phys.*, vol. 94, no. 2, pp. 811–821, Jul. 2003.
[6] C. M. Soukoulis and P. Markos, "Transfer matrix studies of left-handed materials," in *Anderson Localization and Its Ramifications* (Lecture Notes in Physics), vol. 630, T. Brandes and S. Ketteman, Eds. Berlin, Germany: Springer, 2006, pp. 99–108.
[7] O. Pujol and J. P. Pérez, "A synthetic approach to the transfer matrix method in classical and quantum physics," *Eur. J. Phys.*, vol. 28, no. 4, pp. 679–691, Jul. 2007.
[8] C. Jirauschek, "Accuracy of transfer matrix approaches for solving the effective mass Schrödinger equation," *IEEE J. Quantum Electron.*, vol. 45, no. 9, pp. 1059–1067, Sep. 2009.

[9] T. Zhan, X. Shi, Y. Dai, X. Liu, and J. Zi, "Transfer matrix method for optics in graphene layers," *J. Phys., Condens. Matter*, vol. 25, no. 21, May 2013, Art. no. 215301.

[10] M. Zamani, H. N. Hajesmaeili, and M. H. Zandi, "Transfer matrix method-based approach to study the bi-gyrotropic magnetic materials," *Opt. Mater.*, vol. 58, pp. 38–45, Aug. 2016.

[11] D. S. Efremenko, V. M. García, S. G. García, and A. Doicu, "A review of the matrix-exponential formalism in radiative transfer," *J. Quant. Spectrosc. Radiat. Transf.*, vol. 196, pp. 17–45, Jul. 2017.

[12] X. Rui, G. Wang, and J. Zhang, *Transfer Matrix Method for Multibody Systems*. Singapore: Wiley, 2019.

[13] J. Li, X. Zhu, C. Shen, X. Peng, and S. A. Cummer, "Transfer matrix method for the analysis of space-time-modulated media and systems," *Phys. Rev. B, Condens. Matter*, vol. 100, no. 14, Oct. 2019, Art. no. 144311.

[14] L. M. Wedepohl, "Wave propagation in nonhomogeneous multi-conductor systems using the concept of natural modes," *Proc. IEE*, vol. 113, no. 4, pp. 622–626, Apr. 1966.

[15] L. M. Wedepohl and C. Indulkar, "Wave propagation in nonhomogeneous systems: Properties of the chain matrix," *Proc. IEE*, vol. 121, no. 9, pp. 997–1000, Sep. 1974.

[16] D. S. Bethune, "Optical harmonic generation and mixing in multilayer media: Analysis using optical transfer matrix techniques," *J. Opt. Soc. Amer. B, Opt. Phys.*, vol. 6, no. 5, pp. 910–916, May 1989.

[17] J. A. B. Faria and J. F. B. da Silva, "Application of a first-order perturbation method to the analysis of almost periodic multiport network chains," *Archiv Elektrotechnik*, vol. 73, no. 6, pp. 433–441, Nov. 1990.

[18] M. V. D. G. Neves and J. A. B. Faria, "On the discretization process involved in the staircase-approximation technique for analyzing radially inhomogeneous optical fibers," *Microw. Opt. Technol. Lett.*, vol. 6, no. 12, pp. 710–715, Sep. 1993.

[19] J. B. Pendry and P. M. Bell, "Transfer matrix techniques for electromagnetic waves," in *Photonic Band Gap Materials* (NATO ASI Series), vol. 315, C. M. Soukoulis, Ed. Dordrecht, The Netherlands: Springer, 1996, pp. 203–2285.

[20] J. A. B. Faria, "On the transmission matrix of 2*n*-port reciprocal networks," *Microw. Opt. Technol. Lett.*, vol. 33, no. 3, pp. 151–154, May 2002.

[21] J.-H. Kim and M. Swaminathan, "Modeling of multilayered power distribution planes using transmission matrix method," *IEEE Trans. Adv. Packag.*, vol. 25, no. 2, pp. 189–199, May 2002.

[22] J. A. B. Faria and M. G. Neves, "A theoretical analysis of band-edge irregular propagation waves in single-mode fiber Bragg gratings," *J. Opt. Commun.*, vol. 24, no. 5, pp. 165–168, Oct. 2003.

[23] J. A. B. Faria,"Frequency-domain modal analysis of nonuniformly coupled transmission-line structures," *Microw. Opt. Technol. Lett.*, vol. 43, no. 3, pp. 186–189, Nov. 2004.

[24] J. A. B. Faria, "A matrix approach for the evaluation of the internal impedance of multilayered cylindrical structures," *Prog. Electromag. Res. B*, vol. 28, pp. 351–367, Mar. 2011.

[25] J. A. B. Faria, "A circuit approach for the electromagnetic analysis of inhomogeneous cylindrical structures," *Prog. Electromag. Res. B*, vol. 30, pp. 223–238, May 2011.

[26] P. Rulikowski and J. Barrett, "Ultra-wideband pulse shaping using lossy and dispersive nonuniform transmission lines," *IEEE Trans. Microw. Theory Techn.*, vol. 59, no. 10, pp. 2431–2440, Oct. 2011.

[27] R. Aylo, G. Nehmetallah, H. Li, and P. P. Banerjee, "Multilayer periodic and random metamaterial structures: Analysis and applications," *IEEE Access*, vol. 2, pp. 437–450, 2014.

[28] A. Momeni, M. Baharian, and A. Abdolabi, "General analysis of coupled nonuniform transmission lines based on state transition matrix," *IEEE Trans. Electromagn. Compat.*, to be published.

[29] B. H. Song and J. S. Bolton, "A transfer-matrix approach for estimating the characteristic impedance and wave numbers of limp and rigid porous materials," *J. Acoust. Soc. Amer.*, vol. 107, no. 3, pp. 1131–1152, Mar. 2000.

[30] C. Cai, G. Liu, and K. Lam, "A transfer matrix approach for acoustic analysis of a multilayered active acoustic coating," *J. Sound Vib.*, vol. 248, no. 1, pp. 71–89, Nov. 2001.

[31] Y. H. Pao, W. Q. Chen, and X. Y. Su, "The reverberation-ray matrix and transfer matrix analyses of unidirectional wave motion," *Wave Motion*, vol. 44, no. 6, pp. 419–438, Jun. 2007.

[32] A. Morro and G. Caviglia, "Wave propagation in a stratified layer via the matricant," *Commun. Appl. Ind. Math.*, vol. 2, no. 1, p. 367, Aug. 2011.

[33] A. Dijckmans and G. Vermeir, "Development of a hybrid wave based-transfer matrix model for sound transmission analysis," *J. Acoust. Soc. AmER.*, vol. 133, no. 4, pp. 2157–2168, Apr. 2013.

[34] G. Liu, S. Li, Y. Li, and H. Chen, "Vibration analysis of pipelines with arbitrary branches by absorbing transfer matrix method," *J. Sound Vib.*, vol. 332, no. 24, pp. 6519–6536, Nov. 2013.

[35] S. Y. Zhang and M. T. Li, "A simplified transfer matrix method for horizontal seismic response of wall-frame structures considering SSI," *Adv. Mater. Res.*, vol. 1065–1069, pp. 1026–1030, Dec. 2014.

[36] V. B. Teif, "General transfer matrix formalism to calculate DNA-protein-drug binding in gene regulation: Application to OR operator of phage," *Nucleic Acids Res.*, vol. 35, no. 11, P. e80, Jun. 2007.

[37] A. Efremov, R. S. Winardhi, and J. Yan, "Transfer-matrix calculations of DNA polymer micromechanics under tension and torque constraints," *Phys. Rev. E, Stat. Phys. Plasmas Fluids Relat. Interdiscip. Top.*, vol. 94, no. 3, Sep. 2016, Art. no. 032404.

[38] A. Efremov and J. Yan, "Transfer-matrix calculations of the effects of tension and torque constraints on DNA-protein interactions," *Nucleic Acids Res.*, vol. 46, no. 13, pp. 6504–6527, Jul. 2018.

[39] F. R. Gantmacher, *The Theory of Matrices*, vol. 2. New York, NY, USA: Chelsea, 1960.

[40] D. S. Bernstein, *Matrix Mathematics: Theory, Facts, and Formulas*. Princeton, NJ, USA: Princeton Univ. Press, 2005.

[41] J. J. Cunha, "Transition matrix and generalized matrix exponential via the Peano-Baker series," *J. Difference Equ. Appl.*, vol. 11, no. 15, pp. 1245–1264, Dec. 2005.

[42] G. Peano, "Intégration par séries des équations différentielles linéaires," *Math. Ann.*, vol. 32, pp. 450–456, Sep. 1888.

[43] J. E. Campbell, "On a law of combination of operators bearing on the theory of continuous transformation groups," *Proc. London Math. Soc.*, vol. 1, no. 1, pp. 381–390, Nov. 1896.

[44] H. F. Baker, "On the exponential theorem for a simple transitive continuous group and the calculation of the finite equations from the constants of structure," *Proc. London Math. Soc.*, vol. 1, no. 1, pp. 91–129, Mar. 1901.

[45] F. Hausdorff, "Die symbolische Exponentialformel in der Gruppentheorie," *Ber. Verh. Kgl. Sachs. Ges. Wiss. Leipzig. Math.-Phys., Kl.*, vol. 58, pp. 19–48, 1906.

[46] W. Magnus, "On the exponential solution of differential equations for a linear operator," *Commun. Pure Appl. Math.*, vol. 7, no. 4, pp. 649–673, Nov. 1954.

[47] M. Baake and U. Schlagel, "The Peano-Baker series," *Proc. Steklov Inst. Math.*, vol. 275, no. 1, pp. 155–159, 2011.

[48] R. Achiles and A. Bonfigloli, "The early proofs of the theorem of Campbell, Baker, Hausdorff, and Dynkin," *Arch. History Exact Sci.*, vol. 66, no. 3, pp. 295–358, May 2012.

[49] J. A. B. Faria and J. Borges da Silva, "Wave propagation in polyphase transmission lines: A general solution to include cases where ordinary modal theory fails," *IEEE Trans. Power Del.*, vol. 1, no. 2, pp. 182–189, Apr. 1986.

[50] F. Aminifar, M. F. Firuzabad, A. Safdarian, A. Davoudi, and M. Shahidehpour, "Synchrophasor measurement technology in power systems: Panorama and state-of-the-art," *IEEE Access*, vol. 2, pp. 1607–1628, 2014.

[51] J. A. B. Faria and R. Araneo, "A rigorous matrix procedure for calculating the line constants and wave parameters of uniform MTLs using SMT/PMU," *Int. Trans. Elect. Energy Syst.*, vol. 27, no. 10, pp. 1–10, e2377, Oct. 2017.

[52] Y. Zhang, T. Huang, and E. Bompard, "Big data analytics in smart grids: A review," *Energy Informat.*, vol. 1, no. 1, 2018, Art. no. 8.

[53] L. A. Pipes, "Matrix theory of multiconductor transmission lines," *London, Edinburgh, Dublin Philos. Mag. J. Sci.*, vol. 24, pp. 97–113, 1937.

[54] L. M. Wedepohl, "Application of matrix methods to the solution of travelling-wave phenomena in polyphase systems," *Proc. IEE*, vol. 110, no. 12, pp. 2200–2212, Dec. 1963.

[55] J. A. B. Faria, *Multiconductor Transmission-Line Structures: Modal Analysis Techniques*. New York, NY, USA: Wiley, 1993.

[56] C. R. Paul, *Analysis of Multiconductor Transmission Lines*. New York, NY, USA: Wiley, 2008.
[57] J. A. B. Faria, "Multimodal propagation in multiconductor transmission lines," *J. Electromag. Appl.*, vol. 28, no. 14, pp. 1677–1702, Oct. 2014.
[58] J. A. B. Faria, "On the segmentation method used for analyzing nonuniform transmission lines: Application to the exponential line," *Eur. Trans. Elect. Power*, vol. 12, no. 5, pp. 361–368, Sep. 2002.
[59] A. Semlyen, "Some frequency domain aspects of wave propagation on nonuniform lines," *IEEE Trans. Power Del.*, vol. 18, no. 1, pp. 315–322, Jan. 2003.
[60] J. A. B. Faria and R. Araneo, "Computation, properties, and realizability of the characteristic immittance matrices of nonuniform multiconductor transmission lines," *IEEE Trans. Power Del.*, vol. 33, no. 4, pp. 1885–1894, Aug. 2018.
[61] J. A. B. Faria and R. Araneo, "Matching a nonuniform MTL with only passive elements is not always possible," *IEEE Trans. Power Del.*, vol. 34, no. 2, pp. 467–474, Apr. 2019.

**J. A. BRANDÃO FARIA** (Fellow, IEEE) was born in Figueira da Foz, Portugal, in 1952. He received the Ph.D. and Habilitation degrees in electrical engineering from the Instituto Superior Técnico (IST), University of Lisbon, Lisbon, Portugal, in 1986 and 1992, respectively. Since 1994, he has been a Full Professor of electrical engineering with the IST, University of Lisbon, teaching undergraduate courses in electromagnetics and circuit theory, where his research activities are currently carried out with the Instituto de Telecomunicações. He is the author of four books on electrical engineering subjects, including *Análise de Circuitos* (Lisbon: IST Press, 2016), *Electromagnetic Foundations of Electrical Engineering* (Chichester, U.K.: Wiley, 2008), *Óptica* (Lisbon: Ed. Presença, 1995), and *Multiconductor Transmission-Line Structures* (NY, USA: Wiley, 1993). He has published over 120 scientific articles in major peer-reviewed periodicals. His current areas of interest include electromagnetic-field problems, applied electromagnetics, and wave propagation phenomena in multiconductor transmission lines. He was a recipient of the Scientific Prize in Electrical Engineering Research awarded by the University of Lisbon, in 2016.